Mars Shuttle Vehicle and Mission Design
AE 598 Project 2

Karthik Mahesh and Michelle Zosky
Department of Aerospace Engineering, University of Illinois

Preparation for future human exploration missions to Mars is already in progress. A potential contribution to the implementation of these missions is the establishment of a gateway station in orbit around the planet. The station could act as a convenient outpost for transport vehicles to deliver crew and supplies. Crew members and cargo that need to be delivered to the surface can do so with the use of a reusable shuttle designed for sustainable atmospheric entry and exit at Mars. We have designed a vehicle for this very purpose, using certain imposed constraints and assumptions. Though this shuttle is not possible with the current available technology in the industry, advances are underway that may contribute to a realistic vehicle of this nature by the time a human Mars mission becomes a reality. Therefore some of our assumptions include a projection of technological advances, and the corresponding results give insight into the gaps that need to be filled.

Nomenclature

A_{ref}	=	Vehicle Reference/Planform Area (m^2)
A_{wet}	=	Vehicle Wetted Area (m^2)
a_T	=	Thrust Acceleration (m/s^2)
β	=	Ballistic Coefficient (kg/m^2)
C_D	=	Drag coefficient
C_L	=	Lift coefficient
C_p	=	Pressure coefficient
C_{sys}	=	Constant Vehicle Systems Mass
f_{crw}	=	Variable Crew mass (kg per person)
f_{sys}	=	Systems mass per unit dry mass
f_{tank}	=	Tank mass per unit propellant volume (kg/m^3)
f_{tps}	=	Thermal Protection System mass fraction (of vehicle mass)
γ	=	Flight path Angle (deg)
γ_i	=	Flight path Angle at start of gravity turn (deg)
g	=	acceleration due to gravity on Mars (m/s^2)
g_0	=	acceleration due to gravity on Earth (m/s^2)
H	=	Mars scale height (m)
I_{sp}	=	Specific Impulse (s)
I_{str}	=	Structural index (mass per unit wetted area) (kg/m^2)
L/D	=	Lift-to-Drag ratio
m_0	=	Vehicle total mass (kg)

m_p	=	Propellant Mass (kg)
m_{crw}	=	Total crew mass (kg)
m_{dry}	=	Vehicle dry mass (total mass without propellant) (kg)
m_{eng}	=	Propulsion System mass (kg)
m_{str}	=	Structural mass (kg)
m_{sys}	=	Other vehicle system mass (Includes ECLSS, avionics, etc.) (kg)
m_{tank}	=	Tank mass (kg)
m_{tps}	=	Thermal Protection System mass (kg)
μ	=	Mars gravitational parameter (km/s^3)
N_{crw}	=	Number of crew
R_p	=	Planet radius (m)
ρ_{ref}	=	Reference atmosphere density (kg/m^3)
T_{asc}/T_{desc}	=	Ratio of thrust requirements for ascent and descent
TW_{eng}	=	Ratio of engine Thrust to engine mass (N/kg)
V	=	Velocity (m/s)
V_{circ}	=	Circular velocity at entry interface altitude (m/s)
V_0	=	Velocity at entry interface (m/s)
V_i	=	Velocity at start of gravity turn (m/s)
z	=	Altitude (m)
z_i	=	Altitude at start of gravity turn (m)

I. Introduction

Currently, NASA is leading the Artemis program to develop the technologies needed for further human exploration of the Lunar surface, and they will use the experience gained to prepare for future human missions to Mars[1, 2]. The establishment of a Lunar Gateway as part of this program provides us with reasonable confidence that a similar Gateway-style space station could be established in orbit around Mars. To augment the capabilities of such a Mars space station, we propose a shuttle to transport astronauts and cargo to and from the Mars surface. Our design goals include full reusability and sustainability, and we are targeting maximum propellant efficiency within the potential constraints of future developments in vehicle technology. An additional outcome of our analysis is the identification of technology gaps that will need to be filled in order to make this type of mission possible. Johns Hopkins University Applied Physics Lab, with the support of NASA, is already conducting such research through the Lunar Surface Innovation Consortium, which is an international collaboration across all types of institutions and companies in the industry [3].

Our report will detail the sizing, synthesis, and trajectory design of a re-entry/Single-Stage-To-Orbit (SSTO) vehicle designed for the purpose of delivering astronauts and cargo from the space station to the surface of Mars and back. The vehicle is designed as a lifting vehicle loosely based on the Sierra Nevada Dream Chaser. The inclusion of a return to the space station in the requirements posed several unique challenges. The SSTO launch and associated propulsion system requirements greatly increase the mass of the vehicle, requiring entry at a high ballistic coefficient and leading to a very narrow entry corridor.

II. Methodology

A. Mission Design

We used MATLAB to write a simulation for the mission design trajectory because its built-in capabilities lined up well with our solution methods, including a numerical integrator. We are designing the mission at a high level because we are confident that better technology will be developed by the time a human mission to Mars becomes a reality. Thus we made several assumptions to simplify our process and prevent scope creep, including an exponential atmosphere model, constant gravity, and a point mass for Mars. The values used for the planetary parameters can be found in Table 1. Using these assumptions allowed us to utilize the trajectory models and equations covered in our course material written by Dr. Putnam [4].

Table 1: Mars planetary parameter values

Parameter	Value
R_p	$3.396 \times 10^6\ m$
g	$3.71\ m/s$
ρ_{ref}	$0.02\ kg/m^3$
H	$1.11 \times 10^4\ m$
μ	$4.2828 \times 10^4\ km/s^3$

To start, we made the assumption that the gateway station would orbit Mars at a similar orbit as the Mars Reconnaissance Orbiter. The shuttle begins docked at the station, and then performs a Hohmann transfer to the top of Mars's atmosphere, which we assumed to be at an altitude of 130 km. Typically this type of orbit transfer requires two impulse maneuvers, ending in a circular orbit at the desired radius. However, a circular orbit with $\gamma = 0$ is not ideal for entry. In order to achieve a negative γ_0, we targeted the periapse radius for the transfer orbit to be slightly below the top of the atmosphere. We tested the simulation with a range of pariapses to determine which one produces the appropriate initial conditions for more fuel efficient atmospheric entry, resulting in a target pariapse altitude of $z = 129\ km$.

Keeping in line with our goal of minimizing fuel consumption, we are beginning with equilibrium gliding flight for the initial stage of entry. The first step in the process is to perform a small braking maneuver to slow down to circular velocity, because equilibrium glide conditions require a $V_0 \leq V_{circ}$. For this entry stage, the vehicle follows the trajectory described by Equations (1) to (3). We neglect change in mass during this flight until the vehicle turns on the engines to begin a powered descent.

$$\dot{V} = -\frac{\rho\, V^2}{2\beta} - g \sin\gamma \tag{1}$$

$$\dot{\gamma} = \frac{\rho\, V}{2\beta}\left(\frac{L}{D}\right) - \frac{g\ \cos\gamma}{V} + \frac{V\ \cos\gamma}{R_p + z} \tag{2}$$

$$\dot{z} = V \sin\gamma \tag{3}$$

Our method of choosing the point to begin the powered descent involved an analysis of the necessary a_T/g for starting altitudes along the equilibrium glide trajectory using Equation (4), and these values can be found in Figure 1. When the vehicle reaches the optimum altitude, the engines ignite and fire at constant acceleration to perform a gravity turn maneuver. We calculated this trajectory using Equations (5) to (8), which the vehicle follows until it reaches the surface. These transition points can be seen in Figure 2 over the entire descent trajectory. The softer landing enabled by the powered descent is a necessary requirement to safely transport humans.

$$\left(\frac{a_T}{g}\right)^2 + \sin\gamma_i \left(\frac{V_i^2}{2\, z_i\, g}\right)\frac{a_T}{g} - \left[\frac{V_i^2\left(1 + \sin^2\gamma_i\right)}{4\, z_i\, g} + 1\right] = 0 \tag{4}$$

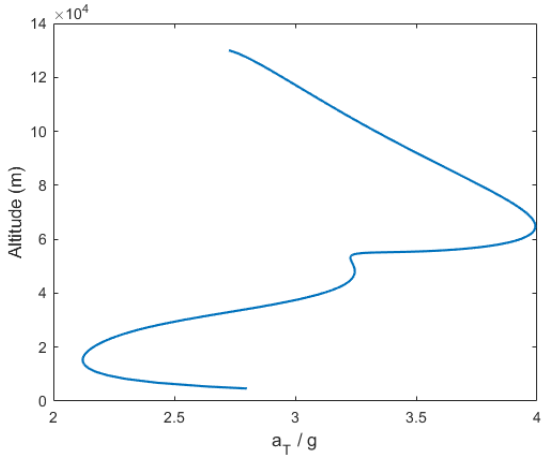

Figure 1: a_T/g required at altitude of gravity turn initiation

$$\dot{V} = -g \sin\gamma - a_T \tag{5}$$

$$\dot{\gamma} = -\left(\frac{g}{V}\right) \cos\gamma \tag{6}$$

$$\dot{m} = -m\left(\frac{a_T}{g_0\, I_{sp}}\right) \tag{7}$$

$$\dot{z} = V \sin\gamma \tag{8}$$

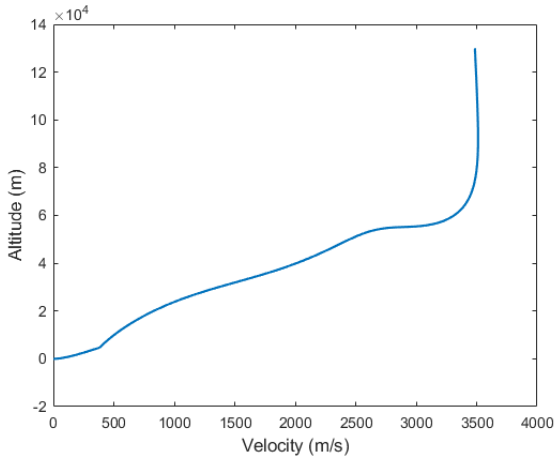

Figure 2: Vehicle velocity against altitude during descent

Once the vehicle completes the mission objectives on the surface, it can make the return journey to the shuttle. We designed the ascent to start vertically and then maneuver to change γ slightly off 90° such that it reaches circular velocity at the top of the atmosphere. We tested a range of values to find an ideal solution, which is discussed in more detail in the Results section.

The ascent trajectory follows Equations (9) to (12), with $\gamma = 0$ at the start, then using the adjusted γ from the transition point. From there, the thrusters turn off so that the vehicle can coast until the gravitational force pulls γ down to zero. Finally, these exit conditions set the vehicle up for a Hohmann transfer back to the gateway orbit.

While running the mission trajectory simulation, we monitored the total fuel required given a range of vehicle parameters, including mass properties, ascent thrust to descent thrust ratio, reference area, ballistic coefficient, drag coefficient, and lift to drag ratio. These parameters were fed into a numerical solver given a window of reasonable values and convergence criteria in order to find a solution. The values that converged directly influenced the vehicle design process.

$$\dot{V} = -g \sin\gamma + a_T \tag{9}$$

$$\dot{\gamma} = -\left(\frac{g}{V}\right) \cos\gamma + \left(\frac{V}{R_p + z}\right) \cos\gamma \tag{10}$$

$$\dot{m} = -m \left(\frac{a_T}{g_0 \, I_{sp}}\right) \tag{11}$$

$$\dot{z} = V \sin\gamma \tag{12}$$

B. Vehicle Design

The vehicle design process was started by freezing the mission requirements that are needed as inputs for vehicle performance. The design mission is simulated to obtain the required propellant mass fraction. Once this is complete, the rest of the vehicle is sized using a variant of the hypersonic convergence method introduced by Czysz and Vandenkerchove [5] and improved by Chudoba et al [6]. The weight methods are slightly modified, while a different volume budget method is used to account for the vehicle configuration being known.

The vehicle configuration, geometry, and aerodynamic analyses are carried out with the help of the Vehicle Sketch Pad parametric geometry tool [7, 8], and an API to use in MATLAB. The geometry is defined around the payload volume and propellant volume. The crew cabin layout is fixed first, inspired by the NASA/ESA Crew Return Vehicle (CRV) [9]. Guidelines on cabin volume are also taken from [5], and the cabin volume requirement sizes the front fuselage. The rear fuselage is sized by propellant and propulsion system volume, and is variable depending on the mass convergence. The wings were initially dimensioned in a similar manner to the wings on the CRV, but the need to increase reference area ended up driving wing sizing.

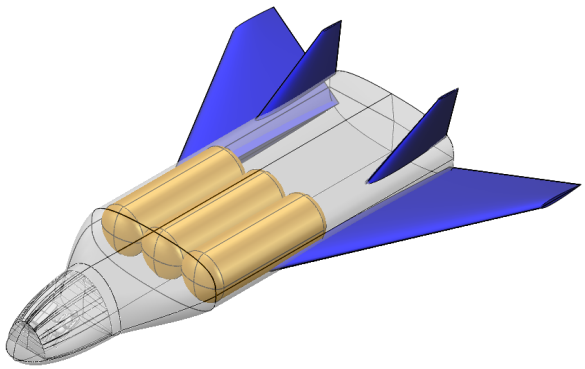

Figure 3: Vehicle 3-D rendering (Engines at rear not modeled)

The aerodynamic analysis is done by importing the vehicle geometry into MATLAB and computing vehicle reference and wetted areas, Newtonian pressure coefficient distribution, lift and drag coefficients, and center of pressure for any

given angle of attack. An example of such a computation can be seen in Figure 4, showing the surface pressure coefficient distribution computed with full Newtonian aerodynamic assumptions. The analysis module was validated against a cone geometry, and values obtained were consistent with the course notes [4]. The center of pressure calculation was included with a view to enable performance and stability analyses, but these items were de-scoped due to the lack of time. The lift and drag analyses have been used as a check for values of aerodynamic coefficients being used in the trajectory design as per Figure 5, while the wetted area plays an important role in the weight budget.

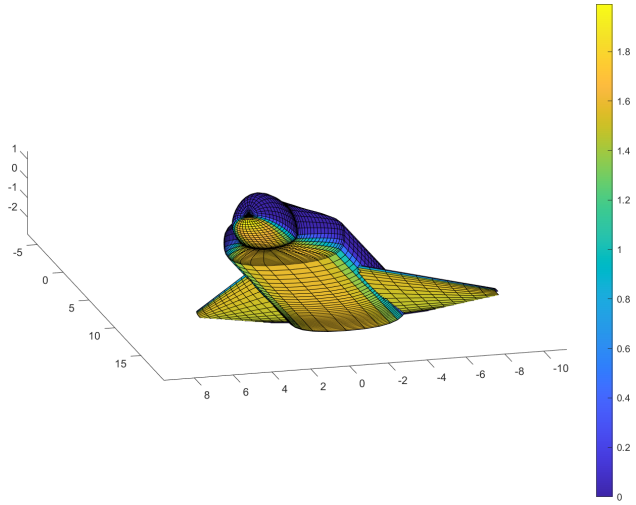

Figure 4: Example of vehicle C_p distribution

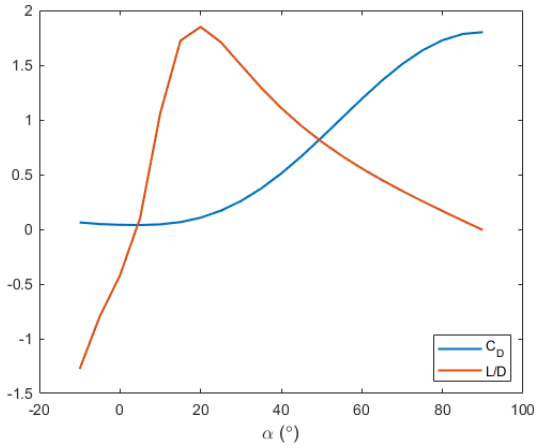

Figure 5: Variation of L/D and C_D with angle of attack

As mentioned earlier, the vehicle weight budget is being computed using a modified version the hypersonic convergence method. The key equations for each component of the dry weight are given in Table 2.

The TPS mass fraction is estimated based on the Space Shuttle's TPS mass fraction, and adjusted downward based on the low heat load expectations on Mars. As can be seen in Table 2, some parameters have much lower values than the

Table 2: Dry weight equations, parameter ranges, and values used [6]

Dry Weight Equations	Parameter Empirical Ranges	Values Used
$m_{str} = I_{str} \times A_{wet}$	$17 \leq I_{str} \leq 23\ kg/m^2$	$I_{str} = 13\ kg/m^2$
$m_{eng} = m_0 \times a_T/TW_{eng}$	$1500 \leq TW_{eng} \leq 2500\ N/kg$	$TW_{eng} = 2400\ N/kg$
$m_{crw} = f_{crw} \times N_{crw}$	$140 \leq f_{crw} \leq 150\ kg/person$	$f_{crw} = 150\ kg/person$
$m_{sys} = C_{sys} + f_{sys} \times m_{dry}$	$0.19 \leq C_{sys} \leq 2.1\ ton$	$C_{sys} = 2.1\ ton$
	$0.16 \leq f_{sys} \leq 0.24\ ton/ton$	$f_{sys} = 0.1\ ton/ton$
$m_{tps} = f_{tps} \times m_0$	$0.03 \leq f_{tps} \leq 0.1$	$f_{tps} = 0.03$
$m_{tank} = f_{tank} \times V_{tank}$		$f_{tank} = 12.0 kg/m^3$

ranges specified in [5, 6]. This is representative of the challenge of keeping weight low in order to make this vehicle possible.

The volume budget is not separately specified here, as most of the configuration layout is being driven by the geometry fixed in OpenVSP. However, the rear fuselage length is driven by the fuel tank volume, and that is reflected in how wetted area changes with weight.

III. Results

During our analysis of the mission trajectory, we found that the adjustment of γ during ascent needed to be 18° pitch down-range (so that $\gamma = 72°$) at an altitude of $z = 148.79\ m$. Figure 6 shows the flight path angles over change in altitude of the remaining trajectory. Another interesting transition to observe is the point in ascent at which the engines are turned off, which can be seen in Figure 7

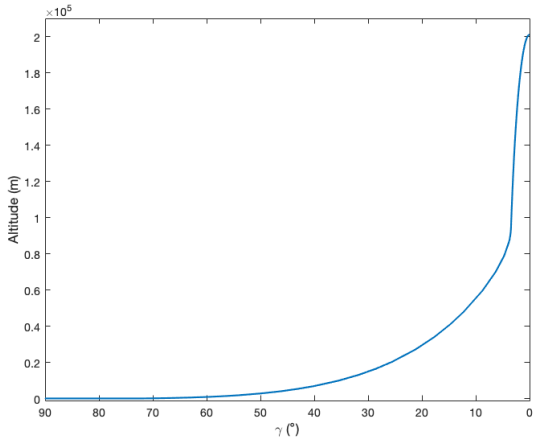

Figure 6: Flight path angle against altitude during ascent

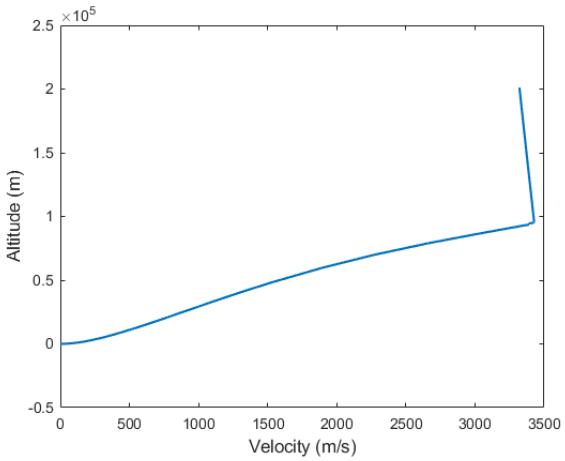

Figure 7: Vehicle velocity against altitude during ascent

We also found that the thrust requirements for descent and ascent are largely similar, which is an improvement on our assumption at the outset that the ascent phase would require 3 to 5 times the thrust of the descent phase. Setting the ascent thrust acceleration equal to the descent thrust acceleration also resulted in a much lower propellant mass fraction. With our final mass values, we were able to track the change in total mass over time during the ascent phase, which corresponds to the fuel spent as seen in Figure 8.

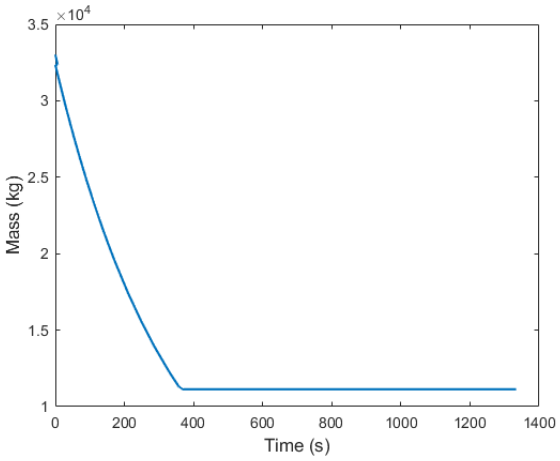

Figure 8: Variation of vehicle mass with time during ascent

With our mission trajectory and vehicle design analysis complete, we found a solution that converged on the set of vehicle parameters in Table 3, which fit within our constraints and assumptions. A more in-depth discussion on the implications of these results is included on the following section.

Table 3: Final vehicle parameter values

Parameter	Value
C_D	1.1
L/D	0.5
A_{ref}	150 m^2
A_{wet}	350 m^2
I_{sp}	360 s
a_T	10.388
a_T/g	2.8
T_{asc}/T_{desc}	1
m_0	3.04×10^4 kg
m_p/m_0	0.7214

IV. Conclusion

While performing the trajectory analysis, we found that achieving entry interface at a near-circular velocity and very small flight path angle (1°) is more propellant-efficient than other approaches using steeper initial flight path angles. However, this approach leaves a very narrow corridor of values for the ballistic coefficient and lift-to-drag ratio that can achieve entry, descent, and a successful soft landing, which played a key role in many other design decisions. The vehicle design started out with an outer mold line inspired by ESA's IXV [10] and the CRV, but as the mission requirement definition progressed, it became clear that the vehicle weight would far exceed initial projections, and the vehicle reference area would have to increase to keep the ballistic coefficient within the narrow range of possible values. This led to the vehicle layout becoming progressively flatter to meet planform area targets, with the final concept seen in Figure 3. It can be seen that despite the small expected payload, the vehicle dimensions are still considerably larger than reentry-only vehicles with comparable payloads.

The ballistic coefficient requirements also enforce extremely futuristic projections for structural weight and crew system weight parameters, as seen in Table 2. A similar effect is seen on the specific impulse of the propulsion system, which uses LOX/RP-1 propellants, and the input specific impulse is 360 s, well beyond the capabilities of current engines. Some sources claim that the current iteration of the SpaceX Merlin 1D has a specific impulse of 348 s, but these sources did not seem credible. A future study could look at the effects of using Methalox or hydrolox propellants insteadon the vehicle weight.

A stability and control analysis was planned but de-scoped due to the lack of time, and this could be taken up as part of future work as well. Another component that we did not consider was orbital rendezvous and cross-range capability analyses, and we anticipate that due to the significant delta-V values required by maneuvers of this kind, including these requirements in the trajectory design might have a significant impact on the final vehicle weight.

We conclude that a spacecraft of this kind may have multiple utilities for human exploration of Mars, but the design

space for the vehicle and trajectory put together is small given the limitations of currently available technology. We hope that given the pace of advancements in space technology, a transportation system like this may become a reality in the future.

Appendix

Our code and simulations can be found in the following GitHub repository: `https://github.com/kmahesh4cheeta/598MarsShuttle/tree/Aero_TrajectoryMods`

Acknowledgments

Our approach to this project began with several brainstorming sessions, during which we each brought ideas and integrated them together to create a cohesive concept that fit our individual interests and skills. We then divided the work into two main components: vehicle design and mission design. Karthik took the lead on the former, while Michelle took the lead on the latter; however we continued to collaborate across the realm of tasks and came together to put everything together throughout the design process. We used GitHub and Overleaf to ensure that we both could utilize our files throughout the design and writing process.

We would like to give acknowledgment and appreciation to Dr. Putnam. His engaging and effective instruction on this course material directly contributed to our success in this project, as well as sparked our interest in the field of planetary entry, descent, and landing systems.

References

[1] NASA, "NASA's Lunar Exploration Program Overview," , 2020. URL `https://www.nasa.gov/sites/default/files/atoms/files/artemis_plan-20200921.pdf`.

[2] Dunbar, B., "What is Artemis?" , Jul 2019. URL `https://www.nasa.gov/what-is-artemis`.

[3] Lab, J. H. U. A. P., "Lunar Surface Innovation Consortium," , 2021. URL `https://lsic.jhuapl.edu/`.

[4] Putnam, Z., "AE 598 Planetary Entry Course Notes," , 2021.

[5] Czysz, P., and Vandenkerchove, J., "Transatmospheric Launcher Sizing," , 1 2001. https://doi.org/10.2514/5.9781600866609.0979.1103.

[6] Simon, S., and Chudoba, B., "Conceptual Design and Sizing Study of Reusable TSTO Launch System," American Institute of Aeronautics and Astronautics, 2021. https://doi.org/10.2514/6.2021-4121, URL https://arc.aiaa.org/doi/10.2514/6.2021-4121.

[7] Hahn, A. S., "Vehicle sketch pad: A parametric geometry modeler for conceptual aircraft design," American Institute of Aeronautics and Astronautics Inc., 2010. https://doi.org/10.2514/6.2010-657.

[8] McDonald, R. A., "Advanced modeling in open VSP," American Institute of Aeronautics and Astronautics Inc, AIAA, 2016. https://doi.org/10.2514/6.2016-3282.

[9] Adams, C. M., Petrov, G., Lévy, F., Ciardullo, C., and Clinton, A., "Optimized architecture for passenger spacecraft," 2008. https://doi.org/10.2514/6.2008-7834.

[10] Zaccagnino, E., Malucchi, G., Marco, V., Drocco, A., Dussy, S., and Préaud, J. P., "Intermediate eXperimental vehicle (IXV), the ESA re-entry demonstrator," 2011. https://doi.org/10.2514/6.2011-6340.